Hyperfine structure of excited alkali states using quantum beat spectroscopy

Hyperfine structure of excited alkali states using quantum beat spectrosopy

W A van Wijngaarden and J Sagle

Department of Physics, York University, Toronto, Ontario M3J 1P3, Canada

Abstract. Quantum beats arising from the hyperfine interaction were observed in the $7D_{3/2} \rightarrow 5P_{1/2}$ transition in ^{85}Rb. Theoretical expressions for the beat signals were fitted to the data to determine the magnetic dipole constant $a = 1.415 \pm 0.030$ MHz, electric quadrupole constant $b = 0.31 \pm 0.06$ MHz and radiative lifetime $\tau = 346 \pm 25$ ns of the ^{85}Rb $7D_{3/2}$ state.

1. Introduction

Quantum beat spectroscopy [1,2] has proved to be a useful tool to determine sub-Doppler energy separations of closely spaced states. We have measured quantum beats arising from the hyperfine structure of excited alkali states [3]. The beats are produced when an initial state that is a linear combination of eigenstates radiatively decays. In our experiment, the rubidium $7D_{3/2}$ state was populated by a two-photon excitation of the $5S_{1/2}$ ground state. Fluorescence was observed when the $7D_{3/2}$ state radiatively decayed to the $5P_{1/2}$ state, as is illustrated in figure 1. The theoretically predicted signals were then fitted to the data to obtain the hyperfine coupling constants as well as the radiative lifetime. In this paper, section 2 gives a brief account of the theory. The apparatus and data analysis are discussed in section 3. Finally, the results are presented and compared to published values in section 4.

2. Theory

A pulsed dye laser excited the rubidium atoms from the $5S_{1/2}$ ground state to the excited $7D_{3/2}$ state. The laser was linearly polarized along the quantization axis z. The excitation was therefore governed by the selection rule $\Delta m_J = 0$, where m_J is the azimuthal quantum number. Hence, only the $m_J = \pm\frac{1}{2}$ Zeeman sub-levels of the $7D_{3/2}$ state, denoted by $|\pm\frac{1}{2}\rangle$, were populated. It is assumed that the laser excitation populates the $\pm\frac{1}{2}$ sub-levels equally. This occurs if the atom is initially unpolarized and if the laser does not resolve the hyperfine levels of the lower and upper states. The hyperfine splitting of the ^{85}Rb ground state is 0.1 cm^{-1}, while the laser linewidth is quoted to be 0.07 cm^{-1} by the manufacturer. We therefore checked the possibility that one of the two hyperfine ground state sub-levels was preferentially excited. This was done by scanning the laser wavelength across the two-photon absorption resonance,
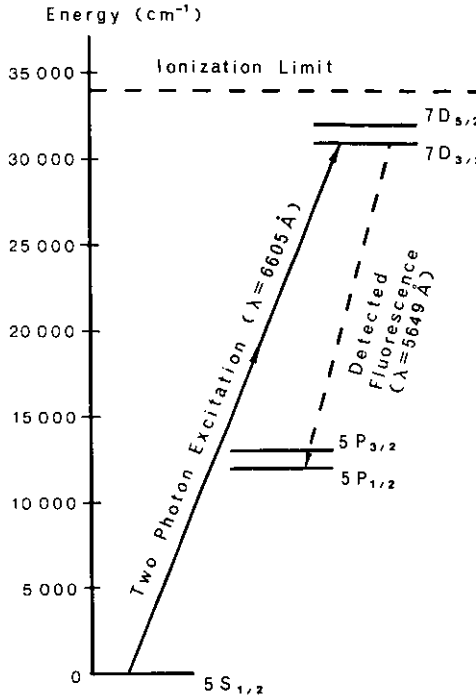
Figure 1. Rubidium energy levels accessed by the experiment.

while monitoring the fluorescence produced by the $7D_{3/2} \rightarrow 5P_{1/2}$ transition. Only a single fluorescence peak was observed showing that the laser excited both of the hyperfine levels of the $5S_{1/2}$ ground state.

The rubidium atom can be accurately modelled as a hydrogenic system since only its outer electron occupies an unfilled shell. The Hamiltonian is given by

$$H = H_0 + ah\boldsymbol{I} \cdot \boldsymbol{J} + bh\frac{[3(\boldsymbol{I} \cdot \boldsymbol{J})^2 + \frac{3}{2}(\boldsymbol{I} \cdot \boldsymbol{J}) - (\boldsymbol{I} \cdot \boldsymbol{I})(\boldsymbol{J} \cdot \boldsymbol{J})]}{2I(2I-1)J(2J-1)} + \mu_B g_J \boldsymbol{J} \cdot \boldsymbol{B} + \mu_B g_I \boldsymbol{I} \cdot \boldsymbol{B}\,. \tag{1}$$

Here H_0 represents the Coulomb and fine structure. The next two terms are the magnetic dipole and electric quadrupole hyperfine interactions, whose magnitude depends on the coupling constants a and b. $\boldsymbol{J}$ is the electronic angular momentum and $\boldsymbol{I}$ is the nuclear spin. The last two terms describe the interaction of the electron and nucleus with an external magnetic field $\boldsymbol{B}$. g_J and g_I are the Lande g-factors of the electron and nucleus respectively and μ_B is the Bohr magneton.

In the absence of a magnetic field, the electronic and nuclear angular momenta are coupled by the hyperfine interaction. The operator $\boldsymbol{I} \cdot \boldsymbol{J}$ transfers atoms back and forth between the Zeeman sub-levels of the excited state. The time dependence of the Zeeman sub-level populations can be monitored by measuring the intensity of polarized fluorescence produced when the excited state radiatively decays. If the excited state Zeeman sub-levels are initially excited anisotropically, temporal oscillations appear in the fluorescent intensity. These oscillations are called quantum beats [1, 2].

The hyperfine eigenstates of the zero field Hamiltonian are denoted by $|JIFm_F\rangle$ where $\boldsymbol{F} = \boldsymbol{J} + \boldsymbol{I}$ is the total angular momentum and m_F is its azimuthal component.

The electronic and nuclear angular momenta are decoupled when an external magnetic field is applied. In the limit of a strong field such that $\mu_B g_J \boldsymbol{J} \cdot \boldsymbol{B}$ is much greater than the hyperfine interaction, the eigenstates are the Zeeman sub-levels. At such large fields [4], there is no exchange of population between the excited state Zeeman sub-levels and we observed no beats in the polarized fluorescence signal.

Detailed reviews of quantum beats have been written by Dodd and Series [1] and by Haroche [2]. They derive expressions for the fluorescent intensity at time t emitted by atoms excited at time $t = 0$. In our experiment, fluorescence produced by the decay of the $7D_{3/2}$ state to the $5P_{1/2}$ state was measured and is given by the following theoretical expression [1, 2, 5, 6]:

$$
I(t) = I_0 e^{-t/\tau} \left\{ \frac{W(J_f, J, 1, 0; 1, J)}{\sqrt{3}[J]^{1/2}} + \frac{W(J_f, J, 1, 2; 1, J)}{\sqrt{6}[I]} \right.
$$

$$
\left. \times P_2(\cos\theta) \sum_{FF'} [F][F'] W^2(1, F, J, 2; J, F') \exp(-\mathrm{i}\omega_{FF'} t) \right\}. \tag{2}
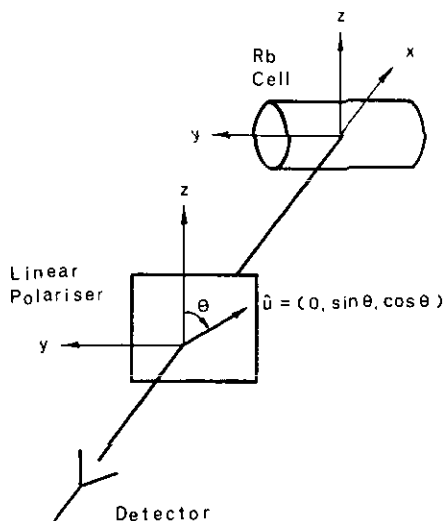$$

Figure 2. Detection of linearly polarized fluorescence. Fluorescence is observed transverse to the laser propagation ($\hat{y}$) and polarization ($\hat{z}$) directions. The linear polarizer transmission axis is oriented along $\hat{u}$.

Here I_0 is a constant proportional to the excited state number density, the finite solid angle of the detector and the transmission efficiency of various optical filters and polarizers. τ is the radiative lifetime of the $7D_{3/2}$ state which has angular momentum $J = \frac{3}{2}$ and decays to the $5P_{1/2}$ state which has angular momentum $J_f = \frac{1}{2}$. W is a Racah coefficient and $[J] = 2J + 1$ is the statistical weight. $P_2(\cos\theta)$ is the second order Legendre polynomial, where θ is the angle between the z direction and the polarization axis of the detected fluorescence as shown in figure 2. $P_2(\cos\theta)$ equals 1, 0 and $-\frac{1}{2}$ when θ equals 0°, 54.7° and 90° respectively. Hence the phase and amplitude
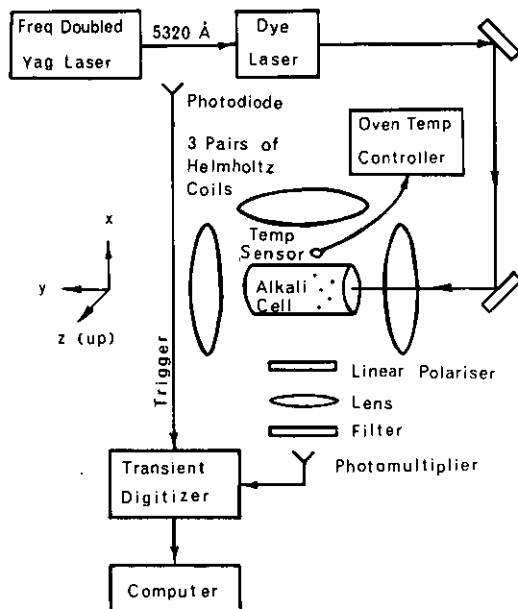
Figure 3. Block diagram of the apparatus used in the experiment.

of the beats depend strongly on the polarization axis of detected light. The frequency $\omega_{FF'} = (E_F - E_{F'})/\hbar$ where

$$E_F = ah\frac{K}{2} + bh\frac{[(3K(K+1) - 4I(I+1)J(J+1)]}{8I(2I-1)J(2J-1)} \tag{3}$$

is the eigenenergy of the state $|JIFm_F\rangle$, and $K = F(F+1) - I(I+1) - J(J+1)$.
Equation (2) can be written to have a simpler appearance as follows:

$$I(t) = I_0 e^{-t/\tau}\left[1 + P_2(\cos\theta)\sum_{FF'} a_{FF'}\cos\omega_{FF'}t\right]. \tag{4}$$

The coefficients $a_{FF'}$ depend on the various angular momenta I, J and J_f, and can be evaluated explicitly from (2). The angular frequencies $\omega_{FF'}$ are functions of the hyperfine coupling constants a and b. In this experiment, the hyperfine constants were found by fitting equation (4) to the data.

3. Experiment

3.1. Apparatus and procedure

The apparatus is shown in figure 3. A dye laser was pumped at a 10 Hz. repetition rate by a frequency doubled Nd:YAG laser. The dye laser wavelength of 6605 Å was chosen to excite the rubidium $5S_{1/2}$ ground state via a two-photon excitation to the $7D_{3/2}$ state. The laser was linearly polarized along the vertical direction. The temporal profile of the laser pulse was measured using a fast photodiode and found to be closely approximated by a Gaussian function having a FWHM of only 7 ns.

The rubidium atoms are contained in a cylindrical pyrex cell having a diameter of 2.54 cm and a length of 25.4 cm. Before the cell was filled with ^{85}Rb, it was simultaneously evacuated by a diffusion pump to a pressure of 1×10^{-7} torr and baked overnight at several hundred degrees Celsius to remove impurities. The cell was located in an oven heated by jets of hot air. A feedback circuit stabilized the temperature to ± 0.1 °C. The entire oven containing the cell was surrounded by three pairs of Helmholtz coils which were used to cancel out the Earth's field. The residual field was measured using a Hall effect Gaussmeter to be less than 10 mG.

Fluorescent light was detected in the direction transverse to both the laser propagation and polarization directions as shown in figure 3. The detected light first passed through a linear polarizer oriented as shown in figure 2. The light was next collimated by a lens onto an interference filter. The filter had maximum transmission at 5647 Å which is the wavelength of light emitted when the rubidium $7D_{3/2}$ state radiatively decays to the $5P_{1/2}$ level. Scattered laser light was blocked since the FWHM bandwidth of the filter was only 10 Å. Finally, the light was focussed onto a photomultiplier (Hamamatsu model R928) which has a (manufacturer quoted) rise time of 2.2 ns. The photomultiplier was contained in a mu-metal housing to shield it from any external magnetic fields. It was operated at sufficiently low voltages to ensure that the output current was linearly proportional to the incoming light intensity. This was checked using a calibrated neutral density filter. Dark current and other sources of background noise were completely negligible. The photomultiplier signal was sent to a transient digitizer (LeCroy Waveform Digitizer 6880A), which was triggered by a fast photodiode that detects the output of the YAG laser. The digitizer had an analogue bandwidth of 400 MHz and digitized the signal every 742 ps. Typically, for a single run, data from 1000 laser pulses were additively accumulated in the digitizer and sent to the computer for analysis.

3.2. Data analysis

Samples of typical data are shown in figure 4. The observed beats were strongly affected by the transmission axis of the linear polarizer in front of the detector as predicted by (4). The beats had the greatest amplitude when vertically polarized light ($\theta = 0°$) was detected and disappeared when $\theta = 54.7°$. Also, the two signals obtained using vertical and horizontal polarizers were observed to be out of phase.

A computer used a least-squares algorithm to fit the following function to the data:

$$S(t) = S_0 e^{-t/\tau} \left[Q + P_2(\cos\theta) \sum_{FF'} a_{FF'} \cos\omega_{FF'} t \right] \qquad (5)$$

where S_0 is an overall scaling factor. The fitted function $S(t)$ does not take into account the finite duration of the laser pulse since this is much less than the observed beat period. Equation (5) has the same form as (4), except for the factor Q. Q is a scaling factor that affects the beat amplitude. It was found to have a value between 2 and 3 indicating that the beats were smaller than expected†. The hyperfine constants a and b were found to be independent of Q. This is not surprising since a and b depend on the beat frequencies $\omega_{FF'}$ and not on the beat amplitudes. Figure 4 shows examples of the very close agreement between the data and the fitted curves.

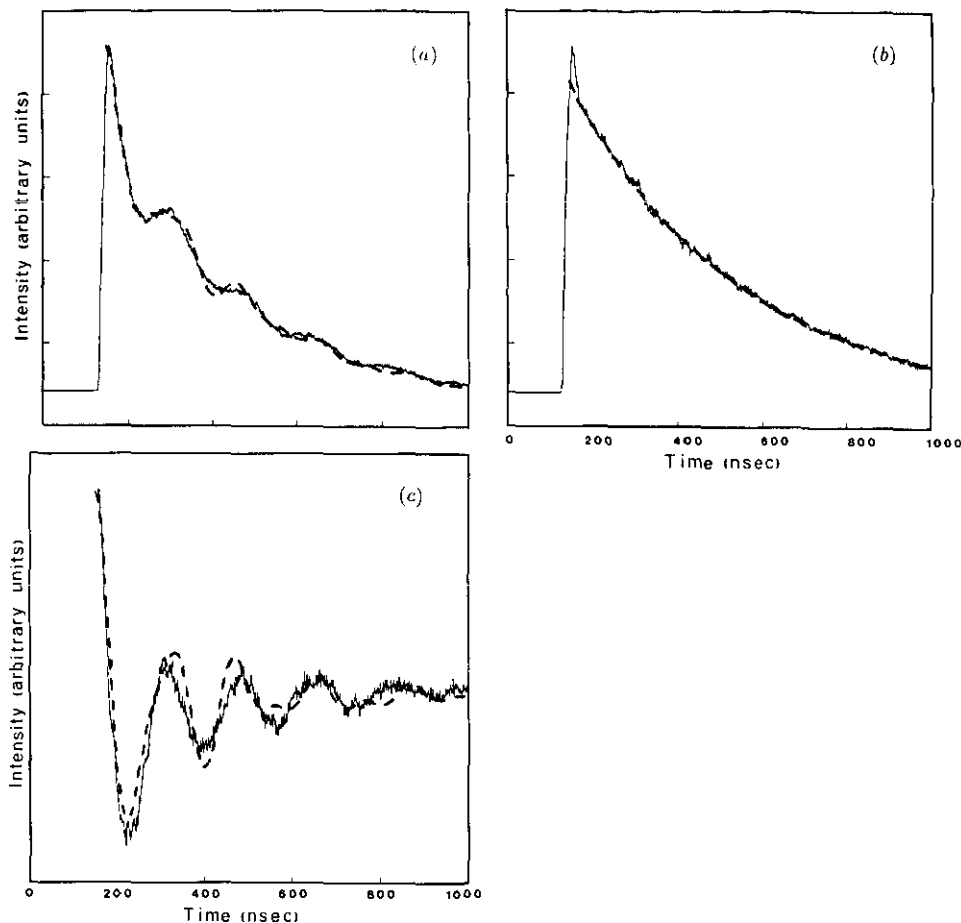† Factors that reduce the amplitude of quantum beats are discussed in [3].

Figure 4. Sample data. Full curves, data; heavy broken curves, theoretical fits. (a) $\theta = 0°$; (b) $\theta = 54.7°$; (c) as (a) except the exponential decay has been subtracted from the data to more clearly show the quantum beats.

The values of the fitted parameters found by averaging the results of dozens of separate runs are recorded in table 1. The error bars are equal to one standard deviation of the best-fit parameters about their mean values. The noise was assumed to be purely statistical since no systematic variation of r, a or b with either cell temperature or laser energy was found. The cell temperature was varied from 80 °C to 120 °C, corresponding to rubidium densities of 10^{12}–10^{13} atoms/cm^3 [7]. Data were taken with laser pulse energies between 1 and 10 mJ.

4. Conclusions

Table 1 lists our measurements of the hyperfine coupling constants of the ^{85}Rb $7D_{3/2}$ state. Our result for the magnetic dipole moment is consistent with that found in [8]. The value for the quadrupole constant b however, disagrees with the result of Svanberg and Tsekeris. The latter used a level crossing experiment [8] to determine the

Table 1. Experimental data for the $7D_{3/2}$ state of ^{85}Rb. a is the magnetic dipole constant, b the electric quadrupole constant and τ the radiative lifetime.

Reference	$|b|$ (MHz)	$|a|$ (MHz)	τ (ns)
Svanberg *et al* [8]		1.34 ± 0.05[a]	
Svanberg and Tsekeris [9]	0.52 ± 0.08[a] $a/b > 0$	1.34 ± 0.01[a]	
Lundberg and Svanberg [10]			388 ± 25
Tsekeris[b] (theoretical calculation)			264
Present work	0.31 ± 0.06 $a/b > 0$	1.415 ± 0.030	346 ± 25

[a] These numbers were found by scaling data taken for ^{87}Rb.
[b] Private communication.

magnitude of the magnetic dipole constant for ^{87}Rb. The same data were apparently re-analysed in 1975 to take into account of the electric quadrupole moment [9]. The electric quadrupole constant should be easier to measure in our experiment since it is about twice as large for ^{85}Rb than for ^{87}Rb.

The lifetime of the $7D_{3/2}$ state was found to be significantly longer than the theoretical estimate. This is consistent with the other experimental measurement made by Lundberg and Svanberg [10]. The theoretical estimate of the lifetime is the result of a Coulomb-approximation calculation [11]. This calculation did not take into account effects such as the core polarization that has been shown to significantly affect computed lifetime values [12]. It will no doubt be of interest to compare future theoretical calculations of radiative lifetimes with experimental results measured with tools such as quantum beats spectroscopy.

References

[1] Dodd J N and Series G W 1978 *Physics of Atoms and Molecules* (New York: Plenum) pp 639–677
[2] Haroche S 1976 *High Resolution Laser Spectroscopy* (New York: Springer) pp 253–313
[3] van Wijngaarden W A, Bonin K D and Happer W 1986 *Phys. Rev.* A **33** 77
[4] van Wijngaarden W A and Sagle J 1991 *Phys. Rev.* A to be published
[5] Blum K 1981 *Density Matrix Theory and Applications* (New York: Plenum)
[6] Frauenfelder H and Steffen R M 1964 *Perturbed Angular Correlations* (Amsterdam: North-Holland)
[7] Nesmeianov A N 1963 *Vapor Pressure of The Elements* (New York: Academic)
[8] Svanberg S, Tsekeris P and Happer W 1973 *Phys. Rev. Lett.* **30** 817
[9] Svanberg S and Tsekeris P 1975 *Phys. Rev.* A **11** 1125
[10] Lundberg H and Svanberg S 1976 *Phys. Lett.* **56A** 31
[11] Bates D R and Damgaard A 1949 *Phil. Trans. R. Soc.* **242** 101
[12] Gruzdev P F and Denisov V I *Opt. Spektrosk.* **52** 15–20